Applied Surface Science 308 (2014) 161–169

Contents lists available at ScienceDirect

Applied Surface Science

journal homepage: www.elsevier.com/locate/apsusc

Electrochemical assisted photocatalytic degradation of salicylic acid with highly ordered TiO_2 nanotube electrodes

Qian Zhang[a], Jinwei Zhu[c], Ying Wang[b], Jiangtao Feng[b], Wei Yan[a,b,*], Hao Xu[b,**]

[a] The State Key Laboratory of Multiphase Flow in Power Engineering, Xi'an Jiaotong University, Xi'an 710049, China
[b] Department of Environmental Science and Engineering, Xi'an Jiaotong University, Xi'an 710049, China
[c] China Aerospace Science and Technology Corporation Fourty-fourth Research Institution, China

ARTICLE INFO

Article history:
Received 5 March 2014
Received in revised form 16 April 2014
Accepted 17 April 2014
Available online 26 April 2014

Keywords:
TiO_2 nanotube arrays (NTs)
Salicylic acid
PPCPs
Photoelectrocatalysis
UV–vis spectroscopy

ABSTRACT

To explore the kinetics of photoelectrocatalytic degradation of salicylic acid, one of the important PPCPs, highly ordered TiO_2 nanotube arrays (NTs) were prepared by the electrochemical anodization and characterized with scanning electron microscopy and X-ray diffraction techniques. The effect of TiO_2 NTs properties, bias potential, initial salicylic acid concentration and solution pH on the degradation efficiency was studied and carefully analyzed. The results revealed that the salicylic acid degradation follows quasi-first order kinetics in the photoelectrocatalytic process, and the fastest decay kinetics was achieved in acidic environment (pH 2). The result was further interpreted through the electrochemical impedance spectroscopy. It is confirmed that the electrochemical assisted photocatalysis is a synergetic approach to combat stable organic substances with improved efficiency.

1. Introduction

During the past two decades, there has been a rising concern about the pharmaceuticals and personal care products (PPCPs) discovered in various surface and ground waters across the world [1,2]. These include a wide variety of chemical substances such as painkillers, antibiotics, tranquilizers, skin care products, hair styling agents and so forth [2]. The discharge of PPCPs and their metabolites into environment through the production process and daily consumption would pose long-term adverse effects, such as gene modification and resistance to drugs, on the aquatic microorganisms and human bodies, even at trace concentrations [3,4]. Besides, due to the continuous usage and release into aquatic environment, the pollution caused by PPCPs usually exhibits the pseudo-persistent behavior [5]. As a consequence, effective removal of such hazardous substance from water system needs to be given priority to avoid any potential toxicity to living organisms.

The conventional wastewater treatment techniques usually show inferior performance in removing these PPCP compounds, such as biological decomposition and physical approaches including adsorption, coagulation and so on [4,6–8]. This is partly ascribed to their anti-bacteria properties, hence PPCPs and their incomplete residues are often detected in the effluent water. Physical methodologies, on the other hand, simply transfer the substances from one phase to another. Therefore, the post treatment steps and associated costs are unavoidable [9].

For decontamination of these recalcitrant and anthropic pollutants with low concentrations (ppm-ppb level), photocatalysis was proved to be an efficient advance oxidation technology [10]. Under band gap illumination, the semiconductor itself can be excited to produce electron (e^-) and hole (h^+) pairs, which will initiate formation of several strong oxidizing radicals such as $^{\bullet}OH$ and $^{\bullet}O_2^-$. These species can non-selectively react with most organics and realize efficient destruction of them [4,11,12]. The photocatalytic decomposition of pharmaceuticals such as non-steroidal anti-inflammatory drugs [13–15], paracetamol [16], fluoroquinolone [17], sulfamethoxazole [18,19], chloramphenicol [20] carbamazepine [21], etc., all demonstrate improved treatment efficiency and lowered toxicity. However, the fast e^-/h^+ recombination rate usually encountered in photocatalysis still retard its further enhancement. In this regard, electrochemical assisted photocatalysis, or photoelectrocatalysis (PEC), which employs a positive bias potential to the semiconductor to keep charge carriers apart by the built-in electric field, has earned increasing attention in recent years [9,22–26].

TiO_2, being a stable, non-toxic and abundant semiconductor, is widely studied as a promising material for remediation of polluted

* Corresponding author at: Department of Environmental Science and Engineering, Xi'an Jiaotong University, Xi'an 710049, China. Tel.: +86 029 82664731.
** Corresponding author.
E-mail addresses: yanwei@mail.xjtu.edu.cn (W. Yan), xuhao@mail.xjtu.edu.cn (H. Xu).

http://dx.doi.org/10.1016/j.apsusc.2014.04.125
0169-4332/

water [27]. The nanostructured TiO_2 developed in recent years even demonstrate superior performance due to the facile charge transport to the electrode surface where interfacial reactions occur. Perpendicular aligned TiO_2 nanotube arrays (TiO_2 NTs), produced by anodic oxidation of titanium substrate, constitute a very important nanostructure in water splitting, solar cells and photocatalysis fields. There are several merits linked with TiO_2 NTs, such as great surface area, strong oxidative power, excellent light penetration and scattering effect and etc. [28]. The most important part lies in its unique nanotubular structure that facilitates photo-excited holes moving towards electrode/electrolyte interface and electrons migrating along the vertical channels towards the titanium substrate [29], thereby leading to a decreased probability of e^-/h^+ recombination. From the practical perspective, the in-situ growth of TiO_2 NTs on titanium substrates facilitates the readily use as photoanodes in wastewater purification, without the need of catalyst separation.

According to the mechanism of photoelectrocatalysis, there are several factors affecting its performances, including external bias potential, light intensity, solution condition, electrode geometry properties and so on [27,30]. PPCPs, being a special type of organics, their degradation behavior subjected to the PEC process are still lack of enough investigation. Salicylic acid (SA), one of the important stock chemicals widely used in production of pharmaceuticals and cosmetics, is selected as our target pollutant due to its serious damage to human health and the aquatic environment [31]. The aim of this work is to understand the factors controlling the photoelectrocatalytic oxidation of salicylic acid over TiO_2 NTs electrodes. Through the electrochemical impedance spectroscopy, the effect of pH value on the degradation process of SA is further interpreted. It is expected that this study would give more insights into the PEC oxidation towards salicylic acid, which might be of crucial significance in understanding the PEC degradation behavior of PPCP chemicals with similar structures.

2. Experimental

2.1. Materials

Salicylic acid, ammonia fluoride (NH_4F), ethylene glycol (EG), sodium sulfate (Na_2SO_4), sodium hydroxide (NaOH) and sulfuric acid (H_2SO_4) were all analytical grade chemicals purchased from Fuchen chemical company (PR China). All these chemicals were used without further purification. Titanium sheets (0.5 mm thick) with purity higher than 99.6% were purchased from Baotai. Co. Ltd, China.

2.2. Fabrication of TiO_2 NTs

Prior to the electrochemical anodization, titanium sheets were cut into pieces with dimension of 2 cm × 4 cm, followed by immersing in aqua-regia for 24 h to remove surface organic contaminants. Then the titanium pieces were ultrasonically cleaned in absolute ethanol and ultrapure water for 15 min, respectively. The electrochemical anodization was conducted in two electrode configuration, with the titanium substrate as working electrode and platinum as counter electrode. The electrolyte was comprised of 0.3 wt% NH_4F, 3 vol% H_2O and ethylene glycol, similar with the formula described in previous literatures [32]. A constant voltage of 50 V provided by the DC power supply (Jiangbo, JBP-15005, China) was applied to the electrodes for 1 h at room temperature to form ordered TiO_2 NTs. The as-prepared TiO_2 NTs samples were ultrasonically cleaned in 0.1 M NaOH solution at frequency of 59 kHz and output power of 160 W (provided by sonicator SG5200HPT, Gutel Ltd. company, PR China), to remove surface deposits. Finally, the samples were annealed in air at 500 °C for 2 h, with ramp rate of 1 °C/min to induce crystallization. Specifically, the TiO_2 NTs were anodized for various durations to obtain various lengths and annealed at different temperatures for comparison.

2.3. Characterization

The annealed TiO_2 NTs samples were characterized by SEM and XRD techniques: the surface morphology was obtained on the JSM-6700F field-emission scanning electron microscopy; the crystal structure of TiO_2 NTs was identified by the X'pert PRO MRD diffractometer using Cu-K_α source (λ = 0.15416 nm), with a scanning angle (2θ) range from 10° to 80°.

2.4. Cyclic voltammetry scans and impedance spectroscopy

All electrochemical and photoelectrochemical experiments were performed in the three electrode configuration, with TiO_2 NTs as the working electrode, platinum foil as the counter electrode, and Ag/AgCl (3 M KCl) electrode (206.2 mV vs. NHE at 25 °C) as reference electrode. Please note that all potentials in this work hereafter are referred to the Ag/AgCl (3 M KCl) electrode. Cyclic voltammetry was tested on Ivium potentiostat (Netherland), in 0.1 M Na_2SO_4 supporting electrolyte and 0.1 M Na_2SO_4 containing 20 ppm salicylic acid, respectively. The scan rate was set to be 50 mV/s. The geometric area of the electrode exposing to the electrolyte was 0.07 cm^2. For photoelectrochemical measurements, the conventional cell was replaced by a quartz cell to allow UV light transmission. The light source was provided by a 365 nm LED with total optical output power of 300 mW cm^{-2}. The three light intensities we adopted in this work are 10% (30 mW cm^{-2}), 20% (60 mW cm^{-2}) and 30% (90 mW cm^{-2}), respectively. The illumination area of TiO_2 NTs was set to be 1 cm^2.

To reveal the interfacial charge transfer kinetics in SA photoelectrocatalytic degradation process, the impedance spectroscopy was conducted on CHI 660D potentiostat (Chenhua, China). The perturbation frequency range was between 1000 Hz and 1 Hz, with amplitude potential of 10 mV applied to the working electrode.

2.5. Photoelectrocatalytic activity tests

All PEC degradation tests of SA were conducted in a home-built quartz cell to allow UV light transmission. The CHI 660D potentiostat (Chenhua, China) was employed to provide constant bias voltages, meanwhile recording the corresponding current. The same electrode configuration with the electrochemistry tests was adopted in the PEC process. The TiO_2 NTs samples were serving as working electrodes, with area roughly around 2 × 2.7 cm^2 immersing in the electrolyte with a fixed volume of 40 mL. The electrolyte was comprised of 0.1 M Na_2SO_4 (as supporting electrolyte) and SA with an initial concentration of 20 ppm. Prior to each PEC degradation run, the TiO_2 NTs working electrode was kept in the electrolyte under darkness for 30 min to ensure adsorption equilibrium. The light source was provided by the 500 W Xenon lamp (Trust tech. Co. Ltd., PR China) in full wavelength range with illumination intensity around 453 mW cm^{-2}. To avoid the heating effect caused by the infrared irradiation, the quartz cell was cooled down by circulating water.

The SA concentration was monitored on the Agilent 8453 UV–vis spectrophotometer. During the PEC process, aliquot was withdrawn from the electrolyte at an interval of 10 min to measure the absorbance change. According to the Lambert-Beer law, the absorbance of standard SA solution with various concentrations was recorded, and plotted against concentration to obtain the calibration curve. In order for comparison, direct photolysis,

photocatalysis (PC) and electrocatalysis (EC) experimental runs were also performed.

3. Results and discussion

3.1. Morphology and crystalline structure

Fig. 1 presents the SEM images of TiO_2 NTs annealed at various temperatures and their corresponding XRD patterns. Although some surface debris was not entirely removed off, nanotubular structures can still be noticed in each image. From 400 °C to 600 °C, there is no significant morphology changes (as shown in Fig. 1a–c), while for TiO_2 NTs annealed at 700 °C, the tube walls get much thicker and the nanotubes stack more compact together (Fig. 1d). Such morphology variation with temperature can be interpreted from the XRD results shown in Fig. 1e. It can be observed that at 400 °C the dominant diffraction peaks are perfectly assigned to anatase (1 0 1), (0 0 4) and (2 0 0) planes (JCPDS number

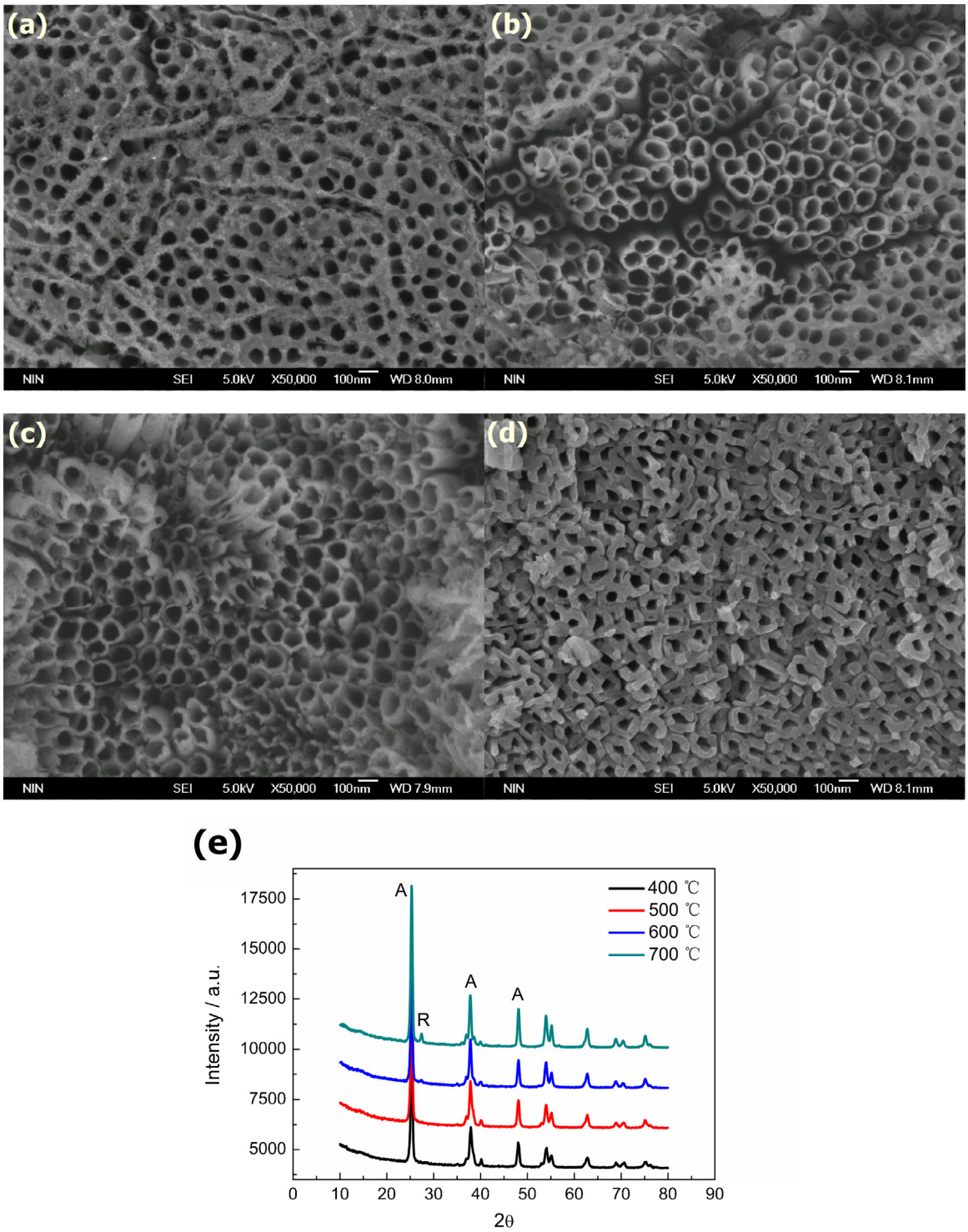

Fig. 1. SEM images of TiO_2 NTs annealed at (a) 400 °C; (b) 500 °C; (c) 600 °C; (d) 700 °C and (e) corresponding XRD patterns of TiO_2 NTs annealed at different temperatures.

Table 1
Crystallite sizes of TiO_2 NTs annealed at various temperatures.

Annealing temperature (°C)	400	500	600	700
Crystallite size (nm)	16.3	16.3	17.1	18.4

00-021-1272). With temperature increases, the intensity of peaks is slightly enhanced, indicating the growth of TiO_2 crystallites. Until the temperature reaches 700 °C, a small diffraction peak at $2\theta = 27.4°$ appears, which suggests the formation of rutile phase TiO_2. Through Sherrer equation, the crystallite sizes of TiO_2 NTs calcined at different temperatures were calculated and listed in Table 1 [33]. It is observed that the crystal dimension increases as temperature rises. Therefore, the tube wall thickening that happens at 700 °C can be ascribed to the large crystallites formed at this temperature. Besides, rutile has a more distorted crystal lattice compared to anatase according to literatures [34]. Hence, the transformation of anatase to rutile may lead to the irregular nanotube geometry.

3.2. Electrochemistry and photoelectrochemistry of TiO_2 NTs

Cyclic voltammetry was employed to study the electrochemical and photoelectrochemical behavior of TiO_2 NTs electrodes in 0.1 M Na_2SO_4 and 0.1 M Na_2SO_4 containing 20 ppm SA, respectively. As presented in Fig. 2a, in 0.1 M Na_2SO_4 electrolyte, extremely small current is detected in the studied potential range without UV illumination. In contrast, under the UV illumination there is a remarkable anodic current rise from around −0.4 V; the current increases significantly as potential sweeps positively, whereas in the cathodic potential range the current remain the same.

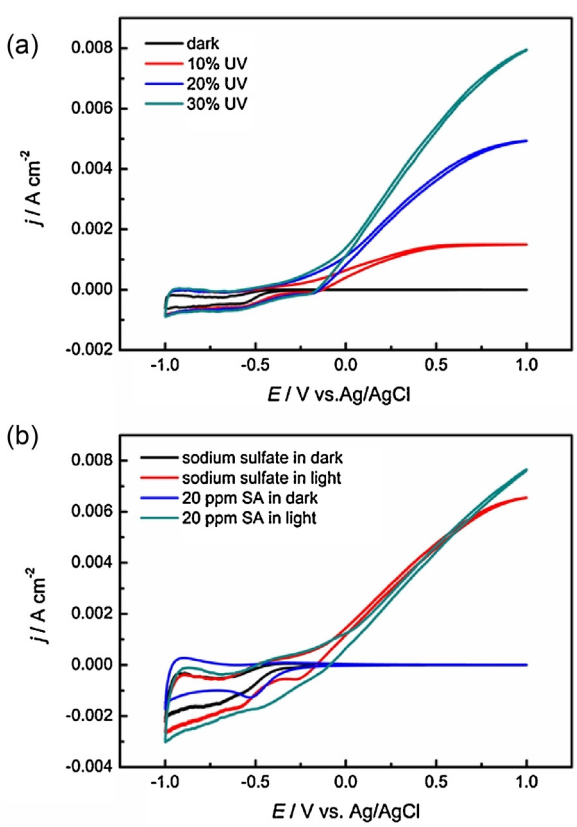

Fig. 2. (a) Cyclic voltammograms of TiO_2 NTs in 0.1 M Na_2SO_4 in the dark and under different UV irradiation intensities; (b) Cyclic voltammograms of TiO_2 NTs in 0.1 M Na_2SO_4 and 0.1 M Na_2SO_4 containing 20 ppm SA, with and without UV irradiation.

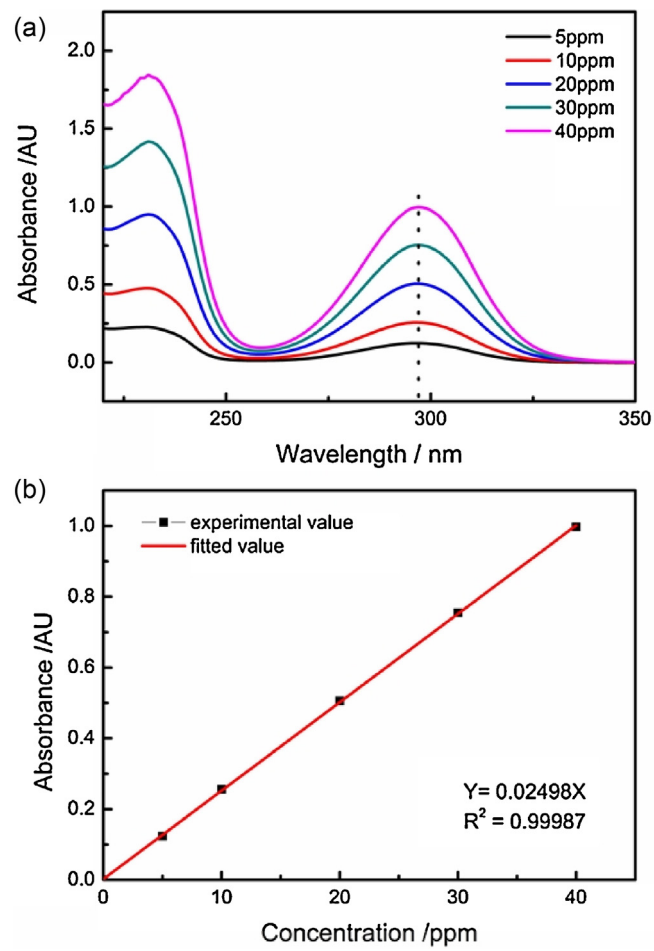

Fig. 3. (a) UV–vis absorption spectra of SA at various concentrations; and (b) the calibration curve of absorbance as a function of SA concentration at 297 nm.

Therefore, it justifies the excellent photo-responsive behavior of TiO_2 NTs under illumination. Another point to note is that the photocurrent saturates at lower anodic potentials with 10% UV irradiation, while the current saturate at more positive potentials with 20% and 30% UV irradiation. This indicates that at low irradiation intensities, the e^-/h^+ charge separation is easily achieved at low bias potential, while the charge separation becomes more difficult as illumination intensity increases. It might be related with the small dimension of TiO_2 nanotube walls where high concentration of e^-/h^+ find difficult to separate apart.

When salicylic acid was added into the 0.1 M Na_2SO_4 electrolyte, as shown in Fig. 2b, there is no measurable photocurrent from −0.4 V in the dark; whereas under illumination the photocurrent is increased and mostly overlapped with that measured in Na_2SO_4 solution without SA, until reaching 0.7 V where the observed photocurrent in SA is slightly higher than that in the background solution. Evidently, there is no so-called photocurrent enhancement effect which is often observed in methanol added electrolyte [35]. It indicates that salicylic acid is a very stable substance that requires high energy to break the chemical bonds. Since cyclic voltammetry is only a dynamic measurement approach, the degradation of SA under constant illumination and bias potential is studied in the following sections.

3.3. Photoelectrocatalytic activity tests

3.3.1. Calibration curve of SA standard solution

Fig. 3 shows the spectral absorbance curves measured at different SA concentrations, and the calibration curve obtained at

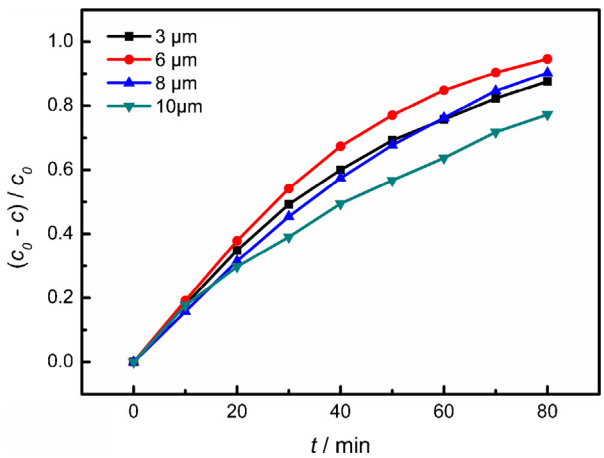

Fig. 4. Effect of TiO_2 NTs length on SA degradation in PEC process at 0.5 V with initial concentration of 20 ppm.

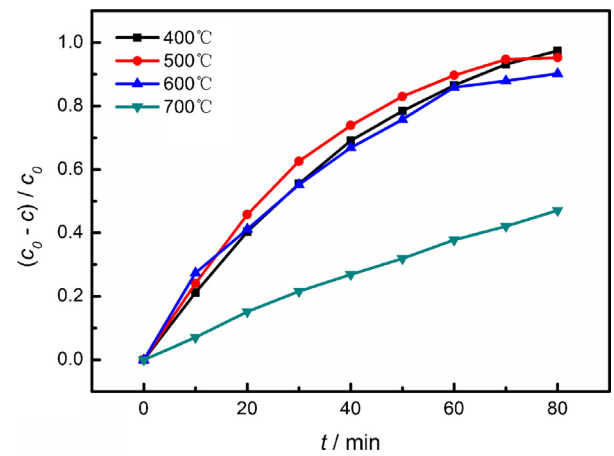

Fig. 5. Effect of TiO_2 NTs calcination temperature on SA degradation in PEC process at 0.5 V with initial concentration of 20 ppm.

wavelength of 297 nm. Clearly, a good linear relationship between the absorbance at 297 nm and SA concentration was established, as the regression coefficient R^2 reaches 0.99987. Thus, in the following SA degradation experiments, the absorbance changes with time at $\lambda = 297$ nm were recorded, and the values were converted into concentrations according to the linear regression equation $y = 0.02498x$ as displayed in Fig. 3b.

3.3.2. Parameters affecting the PEC degradation of SA

3.3.2.1. Effect of TiO_2 NTs electrode properties. Photoelectrochemical oxidation of SA was conducted at potential of 0.5 V and constant illumination of 453 mW cm^{-2}. The effect of TiO_2 NTs electrode properties was first considered. Fig. 4 presents the comparison result of SA degradation achieved on TiO_2 NTs with differing lengths and similar wall thickness. As can be seen, TiO_2 NTs featuring 6 μm long possesses the highest decontamination rate in 80 min while that with 10 μm length exhibits the lowest removal efficiency. The degradation discrepancy between various tube lengths can be explained as follows. In theory, for nanotube structure the surface area is primarily affected by the tube length, so with tube length prolongs the surface area for photon absorption also increases. This is justified by the excellent light penetration and scattering properties found in such regular nano-structures [36,37]. On the other hand, as surface area increases more active sites would be accessible for heterogeneous catalytic reaction to occur, so the improved degradation activity with the increase of tube length is expected. However, the experimental data showed us the inconsistent tendency in SA degradation process; similar results were also obtained in previous reports [38]. It is speculated that beyond a certain range of TiO_2 NTs length, the diffusion of reacting species inside the inner tubes plays a key role in controlling the overall reaction rates.

The effect of TiO_2 NTs annealing temperature on the PEC activity towards SA was investigated as shown in Fig. 5. It can be observed that from 400 °C to 600 °C, the degradation efficiency shows slight discrepancy whereas at 700 °C a significant drop happens. This phenomenon can be explained from the perspective of morphology and crystalline structure of TiO_2 NTs. As shown before, the TiO_2 NTs remained the same micro-appearance from 400 °C to 600 °C, until 700 °C that the shrinkage of nanotubes occurs caused by the crystal grain growth. On the other hand, rutile phase TiO_2 was formed at 700 °C. It is well accepted before that anatase/rutile heterojunction facilitates photo-induced charge separation and high photoactivity [39]. However, this is not the case in our study as shown in Fig. 5 that the SA removal efficiency is significantly lower with rutile TiO_2 formed. One reason could be ascribed to the decreased surface area and non-uniform structure with increasing annealing temperature. Therefore, in this regard, one can conclude that the photoactivity is not only related with crystalline structure, but also closely associated with the micro-morphology. In the following experiments, 6 μm long TiO_2 NTs electrodes annealed at 500 °C were employed to treat SA model pollutant.

3.3.2.2. Effect of external bias potential. Fig. 6 presents the SA removal performance on TiO_2 NTs electrodes at different polarizing potentials. During 2 hour's decomposition, the SA removal ratios for 0.2 V, 0.5 V and 0.8 V are 94.02%, 98.52% and 99.43%, respectively. The increased bias potential results in a slight enhancement in SA degradation rates. As observed from Fig. 2a, the selected external potentials are all positive to the photocurrent onset potential (flatband potential of TiO_2 NTs). Therefore, a band bending and associated potential gradient extends over the TiO_2 NTs nano-structures [40]. However, with the small dimension of TiO_2 nanotube walls (around 15–18 nm), even if the whole nanotubes become depleted, the maximum space charge layer width is around 7–9 nm in our case [29]. Hence, the charge separation at higher voltage conditions is not remarkable, compared to the lower voltage conditions. That explains the reason why little enhancement in SA degradation rates is observed from 0.5 V to 0.8 V. For the following experiments, 0.5 V bias potential was adopted since the SA degradation efficiency at this potential is satisfactory.

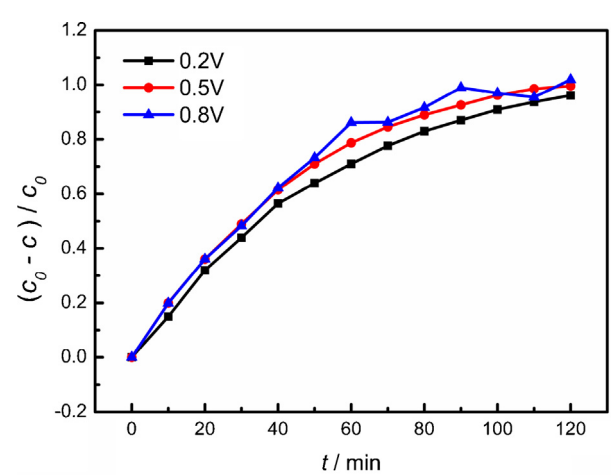

Fig. 6. Effect of bias potential on SA degradation in PEC process with initial concentration at 20 ppm.

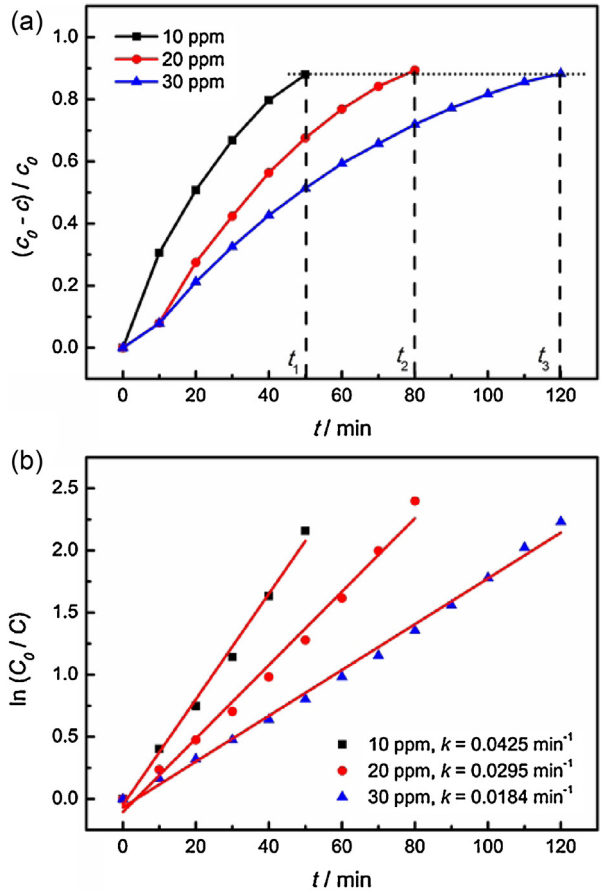

Fig. 7. (a) Comparison of time required for the same degradation efficiency at different initial SA concentrations; and (b) effect of initial SA concentration on its degradation kinetics in PEC process at 0.5 V.

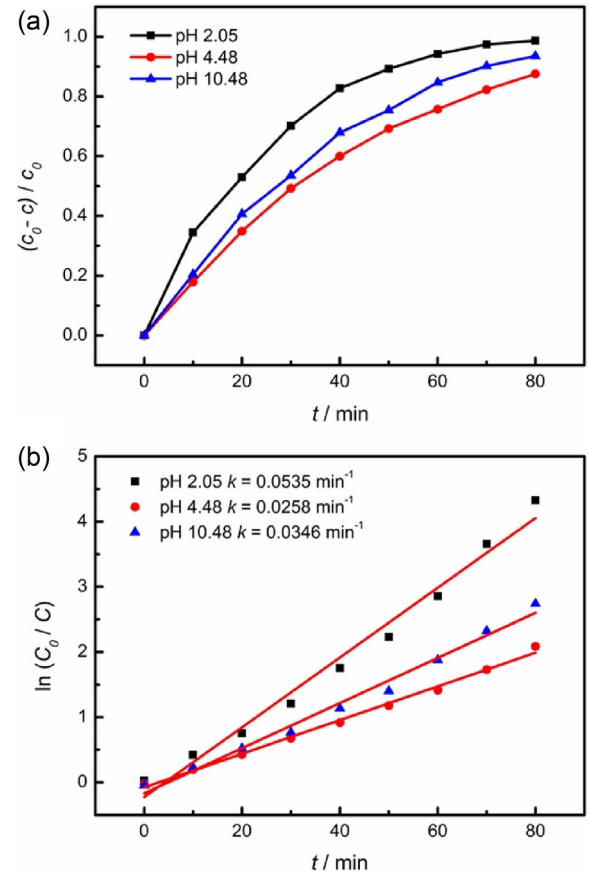

Fig. 8. (a) Effect of pH on SA degradation in PEC process at 0.5 V with initial concentration of 20 ppm; and (b) fitted first order degradation kinetics under different pH conditions.

3.3.2.3. Effect of SA initial concentration and its decay kinetics in PEC process. Fig. 7 shows the SA degradation efficiency with different initial concentrations, and their decay kinetics analyzed by the Langmuir-Hinshelwood model which is often employed to describe photocatalytic kinetics [40,41]. Under specific conditions, the Langmuir-Hinshelwood equation can be simplified into the first order equation shown below:

$$\ln\left(\frac{c_0}{c}\right) = kt \quad (1)$$

where c_0 is initial concentration of SA; c is the SA concentration at t moment; k is the apparent rate constant; and t is reaction time. Fig. 7a presents the degradation efficiency at various SA initial concentrations and it can be seen from the curves that the time required for reaching the same removal ratio follows the sequence of $t_1 < t_2 < t_3$. Using the above mentioned equation (1), we plotted $\ln(c_0/c)$ against t yielding the linear relationship curves shown in Fig. 7b. Evidently, in the SA concentration range we studied, the PEC decomposition of SA follows pseudo first order kinetics. The reaction rate constants were obtained and displayed in the right corner of Fig. 7b. The trend is that the first order rate constant decreases as a function of SA initial concentration increases.

3.3.2.4. Effect of solution pH. In wastewater treatment process, solution pH is a crucial parameter influencing the removal of pollutants. Fig. 8 shows the PEC degradation profiles of SA in different pH environment at the applied potential of 0.5 V. Please note that pH 4.48 is the original pH value of the solution comprised of 20 ppm SA and 0.1 M Na_2SO_4. H_2SO_4 and NaOH (0.1 M) were used to adjust the solution pH. Compared to the original solution, both acidic and alkaline pH values enhance the degradation efficiency, especially at pH 2.05 where 98.64% of SA is decontaminated in 90 min. Fig. 8b gives further information on the SA degradation kinetics, where the fastest decay kinetics achieved at pH 2.05, followed by pH 10.48, and the slowest kinetics was obtained at pH 4.48.

In order to interpret the pH effect on the SA degradation kinetics, the electrochemical impedance spectroscopy was carried out. As shown in Fig. 9, at the applied potential of 0.5 V, only one arc is observed on the EIS plane display. Furthermore, the diameter of the arc is the smallest in the acidic medium, while that becomes larger in the alkaline medium. The diameter of the arc in the solution without pH adjustment is the largest. For electrode/electrolyte interface, the equivalent circuit displayed in Fig. 9b is often applied, where R_s represents the solution resistance, R_{ct} represents charge transfer resistance and C_{dl} is the double layer capacitance. Solution resistance is often reflected in the high frequency domain, where the experimental data is overlapped in our case. This suggests that the solution resistance in different medium is more or less the same. Besides, the external potential was kept constant among these tests, so the double layer capacitance should remain unchanged. Consequently, the only difference among these curves lies in the charge transfer resistance. It is also reported in previous literatures that the only arc turned up in the Nyquist plot is associated with the charge transfer step [42]. So in this regard, it is analyzed that the fast SA decay kinetics at pH 2 is associated with the more facile charge transfer across the interface than in basic medium.

It is well accepted that the surface adsorption of the target reactant is a prerequisite for heterogeneous reaction to occur. Previous studies provide powerful evidences that salicylic acid with carboxyl

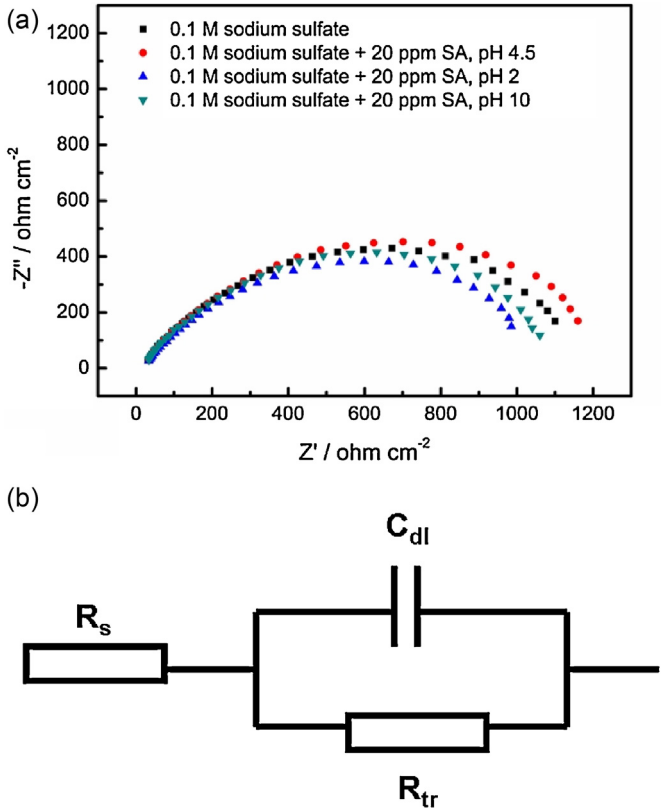

Fig. 9. (a) Nyquist plot of TiO_2 NTs electrodes recorded in 0.1 M Na_2SO_4 electrolyte, and 0.1 M Na_2SO_4 electrolyte with 20 ppm SA at various pH conditions: bias potential 0.5 V, perturbation amplitude 10 mV, frequency range 1000–1 Hz; and (b) equivalent circuit represented by solution resistance R_s, double layer capacitance C_{dl} and interfacial charge transfer resistance R_{ct}.

group is strongly chemisorbed onto TiO_2, forming inner sphere titanium (IV) salicylate surface complexes [43]. Still the affinity of SA to surface titanium ions is remarkably affected by the solution pH. The adsorption quantity of SA on TiO_2 increases with decreasing pH and saturates around 2.5. Besides, since the isoelectric point of TiO_2 is around 5–6 [30,40], at pH 2 the surface of TiO_2 is positively charged, the interaction between SA and TiO_2 surface is even tighter. Therefore, from the chemical point of view, the facile charge transfer in acidic medium is understood. When the solution pH is around 4.5, the SA adsorption quantity decreases and electrostatic interaction becomes weaker, hence the charge transfer gets more difficult. Whereas in alkaline solution (pH 10), the TiO_2 surface is negatively charged and SA is somehow repelled from TiO_2 surface. Under this circumstance, the direct charge transfer from TiO_2 to SA becomes impossible. The coverage of –OH on TiO_2 surface, however, facilitates the generation of •OH radicals which are responsible for SA destruction.

Some researchers found out that the photoxidation rate of SA is insensitive of solution pH, or in other words, independent of SA adsorption quantity [43]. Surface reactive species, on the contrary, is believed to be the great contributor to the overall reaction rate. Since SA is chemisorbed onto TiO_2, the Ti(IV)-salicylate complexes are considered to be the chemical counterparts of surface states [44], so the attack of SA molecules can be achieved through two pathways: (1) hole capture by surface adsorbed hydroxyl groups forming •OH radicals that initiate destruction process; (2) direct hole injection to inner sphere salicylate complexes. When the solution pH is around 2, the degradation proceeds mainly through pathway (2), where chemisorbed salicylate as a deeper hole trap, favors direct hole transfer reaction. On the other hand, at pH 10.48 the distribution of TiOH on TiO_2 surface is greater than 80%, so PEC

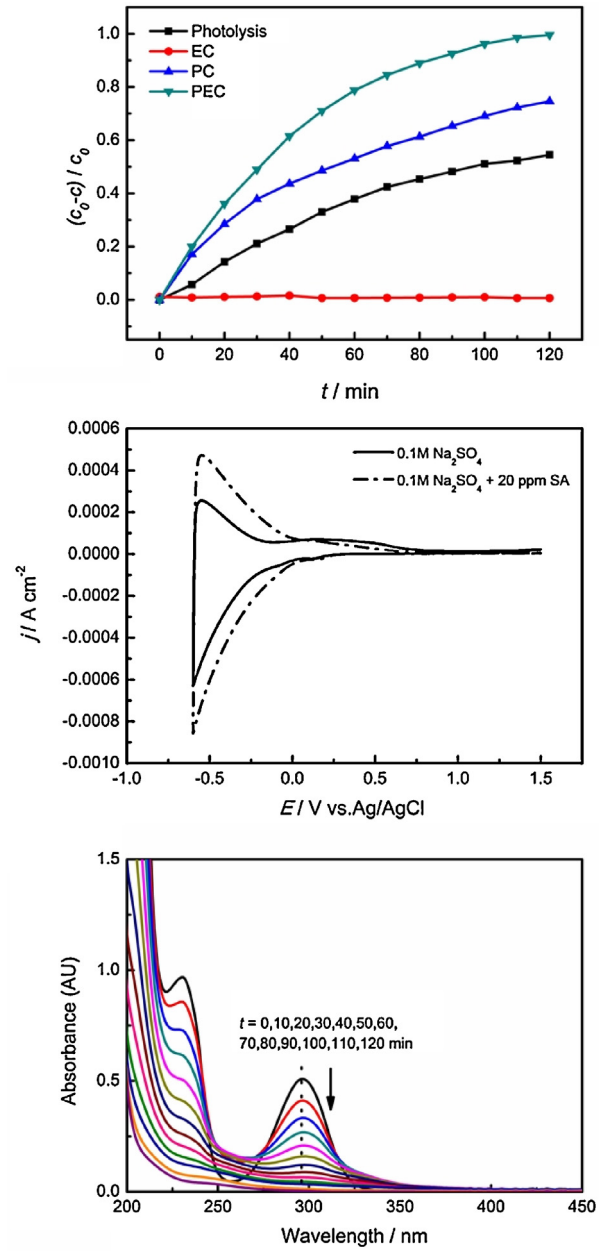

Fig. 10. (a) Comparison of SA degradation ratios under different situations; c_0 is initial concentration of SA; c is the SA concentration at t moment; (b) cyclic voltammetry scans of TiO_2 NTs in 0.1 M Na_2SO_4 supporting electrolyte and 20 ppm SA containing electrolyte at a scan rate of 50 mV/s; and (c) UV–vis absorbance changes of SA with time in the PEC process.

oxidation of SA is mainly via •OH attack. Both these two pH conditions are favorable for the destruction of SA molecules, but the acidic medium promotes faster degradation of salicylic acid.

3.3.3. *Comparison of direct photolysis, PC, EC and PEC processes*

For comparison, the SA decomposition (20 ppm without pH adjustment) under the condition of direct photolysis, photocatalytic process and electrocatalytic process were also carried out shown in Fig. 10. The TiO_2 NTs annealed at 500 °C were served as photocatalysts or working electrodes. In all cases except EC, the irradiation intensity was kept the same and continuous, and in EC and PEC processes a constant bias of 0.5 V was applied. As observed from Fig. 10a, the electrocatalytic oxidation has nearly no decontamination effect on salicylic acid. This is because TiO_2 is n-type semiconductor, so that in the dark there are few holes

that can react with surface adsorbed –OH or water molecules to form •OH. Therefore, no efficient oxidizing agents are produced to destruct SA. On the other hand, salicylic acid, being a very stable aromatic carboxylic acid, requires 28 electrons transferred to be fully mineralized [45]. This means that a high energy barrier needs to be conquered to achieve efficient removal of SA. At the present electrocatalytic conditions, 0.5 V is far from enough to provide adequate energy to decompose SA. Fig. 10b compares the dark cyclic voltammograms over TiO_2 NTs electrodes in 0.1 M Na_2SO_4 supporting electrolyte with and without 20 ppm SA. It is noticed that the current density is increased in the SA containing electrolyte, which could be due to the strong chemisorption property of SA on TiO_2 [45]. Compared to the EC process, the light irradiation plays a significant role in decomposing SA, as indicated in Fig. 3a where the photolysis of SA reaches 55.75% in 2 h. This might be associated with the sensitive properties of SA towards visible light. The removal efficiency is further enhanced in the photocatalytic treatment with 74.32% of SA being degraded. The best treatment performance is achieved in the PEC process where nearly 100% SA is decomposed within 2 h. Fig. 10b provides further spectral evidence that the characteristic peak of SA centered at 297 nm is totally vanished; furthermore, no new peaks are formed indicating the effective destruction of possible intermediates.

Through these control experiments, it is confirmed that photoelectrocatalytic oxidation is an efficient and promising method to decompose stable organic substances. The photoelectrocatalysis is a synergetic approach which combines the photocatalysis to produce highly oxidative radicals and, on the other hand, electric field to separate charge carriers apart and promote the diffusion of reactive species in the solution.

4. Conclusions

In this work, highly ordered TiO_2 NTs was prepared to investigate the photoelectrocatalytic degradation of salicylic acid, one of the representative PPCP chemicals. The prepared TiO_2 NTs were characterized by SEM, XRD, electrochemical and photoelectrochemical techniques. Compared with photocatalysis, photolysis and electrocatalysis, PEC achieved the best performance which could be ascribed to the synergetic effect of light irradiation and external electric field. The effect of TiO_2 properties, bias potential, initial SA concentration and solution pH on PEC degradation of salicylic acid was investigated. It was found that solution pH is a critical factor influencing the degradation rates, with pH 2 as the best favorable condition, followed by pH 10 and subsequently pH 4.5 which is close to the isoelectric point of TiO_2. Electrochemical impedance spectroscopy was employed to account for such results from the perspective of interfacial charge transfer resistance. Finally, it was analyzed that the PEC degradation of salicylic acid exhibits quasi-first order kinetics.

Acknowledgements

The authors gratefully acknowledge the financial support from National Natural Science Foundation of China (Grant No.21307098), China Postdoctoral Science Foundation (2013M532053), and the Fundamental Research Funds for the Central Universities of China. Special thanks are given to technician Zhuang Miao in Northwest Institute for Non-ferrous Metal Research for kindly help in SEM images.

References

[1] G.R. Boyd, H. Reemtsma, D.A. Grimm, S. Mitra, Pharmaceuticals and personal care products (PPCPs) in surface and treated waters of Louisiana, USA and Ontario, Canada, Sci. Total Environ. 311 (2003) 135–149.
[2] C.G. Daughton, Pharmaceuticals and personal care products in the environment: overarching issues and overview, in: ACS Symposium Series, ACS Publications, 2001, pp. 2–38.
[3] S.B. DUCEY, A. SAPKOTA, Presence of pharmaceuticals and personal care products in the environment-a concern for human health? in: ACS Symposium Series, Oxford University Press, 2010, pp. 345–365.
[4] I. Sirés, E. Brillas, Remediation of water pollution caused by pharmaceutical residues based on electrochemical separation and degradation technologies: a review Environ. Int. 40 (2012) 212–229.
[5] G.M. Bruce, R.C. Pleus, S.A. Snyder, Toxicological relevance of pharmaceuticals in drinking water, Environ. Sci. Technol. 44 (2010) 5619–5626.
[6] M.M. Huber, S. Canonica, G.-Y. Park, U. von Gunten, Oxidation of pharmaceuticals during ozonation and advanced oxidation processes, Environ. Sci. Technol. 37 (2003) 1016–1024.
[7] S.K. Khetan, T.J. Collins, Human pharmaceuticals in the aquatic environment: a challenge to green chemistry, Chem. Rev. 107 (2007) 2319–2364.
[8] T.A. Ternes, A. Joss, H. Siegrist, Peer reviewed: scrutinizing pharmaceuticals and personal care products in wastewater treatment, Environ. Sci. Technol. 38 (2004) 392A–399A.
[9] R. Daghrir, P. Drogui, A. Dimboukou-Mpira, M. El Khakani, Photoelectrocatalytic degradation of carbamazepine using Ti/TiO_2 nanostructured electrodes deposited by means of a pulsed laser deposition process, Chemosphere 93 (2013) 2756–2766.
[10] J.H. Carey, J. Lawrence, H.M. Tosine, Photodechlorination of PCB's in the presence of titanium dioxide in aqueous suspensions, Bull. Environ. Contamin. Toxicol. 16 (1976) 697–701.
[11] Z. Liu, X. Zhang, S. Nishimoto, T. Murakami, A. Fujishima, Efficient photocatalytic degradation of gaseous acetaldehyde by highly ordered TiO_2 nanotube arrays, Environ. Sci. Technol. 42 (2008) 8547–8551.
[12] R. Andreozzi, L. Campanella, B. Fraysse, J. Garric, A. Gonnella, R. Lo Giudice, R. Marotta, G. Pinto, A. Pollio, Effects of advanced oxidation processes(AOPs) on the toxicity of a mixture of pharmaceuticals, Water Sci. Technol. 50 (2004) 23–28.
[13] L. Pérez-Estrada, M. Maldonado, W. Gernjak, A. Agüera, A. Fernández-Alba, M. Ballesteros, S. Malato, Decomposition of diclofenac by solar driven photocatalysis at pilot plant scale, Catal. Today 101 (2005) 219–226.
[14] P. Calza, V. Sakkas, C. Medana, C. Baiocchi, A. Dimou, E. Pelizzetti, T. Albanis, Photocatalytic degradation study of diclofenac over aqueous TiO_2 suspensions, Appl. Catal. B: Environ. 67 (2006) 197–205.
[15] F. Méndez-Arriaga, S. Esplugas, J. Giménez, Photocatalytic degradation of non-steroidal anti-inflammatory drugs with TiO_2 and simulated solar irradiation, Water Res. 42 (2008) 585–594.
[16] L. Yang, L.E. Yu, M.B. Ray, Degradation of paracetamol in aqueous solutions by TiO_2 photocatalysis, Water Res. 42 (2008) 3480–3488.
[17] T. Paul, P.L. Miller, T.J. Strathmann, Visible-light-mediated TiO_2 photocatalysis of fluoroquinolone antibacterial agents, Environ. Sci. Technol. 41 (2007) 4720–4727.
[18] M. Abellán, B. Bayarri, J. Giménez, J. Costa, Photocatalytic degradation of sulfamethoxazole in aqueous suspension of TiO_2, Appl. Catal. B: Environ. 74 (2007) 233–241.
[19] P. Calza, C. Medana, M. Pazzi, C. Baiocchi, E. Pelizzetti, Photocatalytic transformations of sulphonamides on titanium dioxide, Appl. Catal. B: Environ. 53 (2004) 63–69.
[20] A. Chatzitakis, C. Berberidou, I. Paspaltsis, G. Kyriakou, T. Sklaviadis, I. Poulios, Photocatalytic degradation and drug activity reduction of chloramphenicol, Water Res. 42 (2008) 386–394.
[21] R. Liang, A. Hu, W. Li, Y.N. Zhou, Enhanced degradation of persistent pharmaceuticals found in wastewater treatment effluents using TiO_2 nanobelt photocatalysts, J. Nanoparticle Res. 15 (2013) 1–13.
[22] A. Zhang, M. Zhou, L. Liu, W. Wang, Y. Jiao, Q. Zhou, A novel photoelectrocatalytic system for organic contaminant degradation on a TiO_2 nanotube (TNT)/Ti electrode, Electrochim. Acta 55 (2010) 5091–5099.
[23] R. Daghrir, P. Drogui, I. Ka, M.A. El Khakani, Photoelectrocatalytic degradation of chlortetracycline using Ti/TiO_2 nanostructured electrodes deposited by means of a Pulsed Laser Deposition process, J. Hazard. Mater. 199 (2012) 15–24.
[24] Y. Liu, X. Gan, B. Zhou, B. Xiong, J. Li, C. Dong, J. Bai, W. Cai, Photoelectrocatalytic degradation of tetracycline by highly effective TiO_2 nanopore arrays electrode, J. Hazard. Mater. 171 (2009) 678–683.
[25] J.H. Li, S.B. Lv, Y.B. Liu, J. Bai, B.X. Zhou, X.F. Hu, Photoeletrocatalytic activity of an n-ZnO/p-Cu_2O/n-TNA ternary heterojunction electrode for tetracycline degradation, J. Hazard. Mater. 262 (2013) 482–488.
[26] C. Liu, D. Fu, H. Li, Behaviour of multi-component mixtures of tetracyclines when degraded by photoelectrocatalytic and electrocatalytic technologies, Environ. Technol. 33 (2012) 791–799.
[27] Y. Zhang, X. Xiong, Y. Han, X. Zhang, F. Shen, S. Deng, H. Xiao, X. Yang, G. Yang, H. Peng, Photoelectrocatalytic degradation of recalcitrant organic pollutants using TiO_2 film electrodes: an overview, Chemosphere 88 (2012) 145–154.
[28] C.A. Grimes, G.K. Mor, Fabrication of TiO_2 nanotube arrays by electrochemical anodization: four synthesis generations, in: TiO_2 Nanotube Arrays, Springer, 2009, pp. 1–66.
[29] X. Wu, Y. Ling, L. Liu, Z. Huang, Enhanced photoelectrocatalytic degradation of methylene blue on smooth TiO_2 nanotube array and its impedance analysis, J. Electrochem. Soc. 156 (2009) K65–K71.
[30] R. Daghrir, P. Drogui, D. Robert, Photoelectrocatalytic technologies for environmental applications, J. Photochem. Photobiol. A: Chem. 238 (2012) 41–52.

[31] M. Tian, B. Adams, J. Wen, R. Matthew Asmussen, A. Chen, Photoelectrochemical oxidation of salicylic acid and salicylaldehyde on titanium dioxide nanotube arrays, Electrochim. Acta 54 (2009) 3799–3805.
[32] Q. Zhang, H. Xu, W. Yan, Fabrication of a composite electrode: CdS decorated Sb–SnO_2/TiO $_2$-NTs for efficient photoelectrochemical reactivity, Electrochim. Acta 61 (2012) 64–72.
[33] J.T. Langford, A. Wilson, Scherrer after sixty years: a survey and some new results in the determination of crystallite size, J. Appl. Crystallogr. 11 (1978) 102–113.
[34] L. Kavan, M. Grätzel, S. Gilbert, C. Klemenz, H. Scheel, Electrochemical and photoelectrochemical investigation of single-crystal anatase, J. Am. Chem. Soc. 118 (1996) 6716–6723.
[35] Z. Zhang, Y. Yuan, Y. Fang, L. Liang, H. Ding, G. Shi, L. Jin, Photoelectrochemical oxidation behavior of methanol on highly ordered TiO_2 nanotube array electrodes, J. Electroanal. Chem. 610 (2007) 179–185.
[36] H.-F. Zhuang, C.-J. Lin, Y.-K. Lai, L. Sun, J. Li, Some critical structure factors of titanium oxide nanotube array in its photocatalytic activity, Environ. Sci. Technol. 41 (2007) 4735–4740.
[37] C.A. Grimes, G.K. Mor, TiO_2 nanotube arrays, Synth. Prop. Appl. (2009).
[38] H.-c. Liang, X.-z. Li, Effects of structure of anodic TiO_2 nanotube arrays on photocatalytic activity for the degradation of 2,3-dichlorophenol in aqueous solution, J. Hazard. Mater. 162, 2009, 1415–1422.
[39] D. Jiang, S. Zhang, H. Zhao, Photocatalytic degradation characteristics of different organic compounds at TiO_2 nanoporous film electrodes with mixed anatase/rutile phases, Environ. Sci. Technol. 41 (2006) 303–308.
[40] M.V.B. Zanoni, J.J. Sene, M.A. Anderson, Photoelectrocatalytic degradation of Remazol Brilliant Orange 3R on titanium dioxide thin-film electrodes, J. Photochem. Photobiol. A: Chem. 157 (2003) 55–63.
[41] Y.R. Smith, A. Kar, V. Subramanian, Investigation of physicochemical parameters that influence photocatalytic degradation of methyl orange over TiO_2 nanotubes, Ind. Eng. Chem. Res. 48 (2009) 10268–10276.
[42] H. Liu, X. Li, Y. Leng, W. Li, An alternative approach to ascertain the rate-determining steps of TiO_2 photoelectrocatalytic reaction by electrochemical impedance spectroscopy, J. Phys. Chem. B 107 (2003) 8988–8996.
[43] A.E. Regazzoni, P. Mandelbaum, M. Matsuyoshi, S. Schiller, S.A. Bilmes, M.A. Blesa, Adsorption and photooxidation of salicylic acid on titanium dioxide: a surface complexation description, Langmuir 14 (1998) 868–874.
[44] W.H. Leng, Z. Zhang, J.Q. Zhang, C.N. Cao, Investigation of the kinetics of a TiO_2 photoelectrocatalytic reaction involving charge transfer and recombination through surface states by electrochemical impedance spectroscopy, J. Phys. Chem. B 109 (2005) 15008–15023.
[45] P. Mandelbaum, S.A. Bilmes, A.E. Regazzoni, M.A. Blesa, The influence of applied bias potential on the photooxidation of methanol and salicylate on titanium dioxide films, Solar Energy 65 (1999) 75–80.